Materials Research Proceedings **22** (2022) 28-34 https://doi.org/10.21741/9781644901878-5

Theoretical Investigation of Ballistic Electron Transport in Au and Ag Nanoribbons

Sushil Kumar[a] and R.K. Moudgil[b*]

Department of Physics, Kurukshetra University, Kurukshetra – 136 119, Haryana, India

[a]smutreja619@gmail.com, [b]rkmoudgil@kuk.ac.in

Keywords: Electron Transport, Nanoribbons, DFT, NEGF, Thermoelectric

Abstract. We have systematically investigated the ballistic electron transport in gold and silver nanoribbons using first principle methods. The electronic structure calculation is carried out using the "density functional theory" (DFT) within the "SIESTA" code. While the electronic transport is studied using the "non-equilibrium Green's function" (NEGF) method combined with the "Landauer-Buttiker" (LB) approach. We have explored the transport along both the armchair (AC) and zigzag (ZZ) directions. Interestingly, both elements turn semiconducting in the AC-configuration, and their band gap oscillates with increasing width of the nanoribbon. On the other hand, nanoribbons retain metallic character in the ZZ-configuration, with a quantized electrical conductance $4G_0$ for sufficiently small width and temperatures as high as nearly 200 K; $G_0=2e^2/h$, is the elementary quanta of electrical conductance. At zero bias, electronic thermal conductance in each system increases non-linearly with temperature. More is the width of nanoribbons, more is the electronic contribution to heat transport. Further, to assess the utility of nanoribbons in thermoelectric devices, we have calculated the room-temperature Seebeck coefficient S. It is found to evince an oscillatory structure as a function of electrochemical potential μ of electrodes, with pronounced peaks (nearly -118 μV/K in the narrowest gold nanoribbon considered) in the AC-configuration. The maximum S achieved is seen to be comparable to the atomic chains of these elements in linear, ladder and zigzag topologies, suggesting practical importance of nanoribbons as thermoelectric sensors in nanoelectronic devices.

Introduction

One dimensional (1D) materials (viz. atomic chains, nanoribbons, nanorods, etc.) have emerged as an exciting field of research during last few decades. These materials have width and/or thickness in nanometer range and consequently, they show dramatically modified electronic structure due to pronounced quantum confinement effect along the nanoscale dimensions. Owing to this, 1D materials show interesting and unusual electronic properties like ballistic electron transport, quantized electrical conductance, quantum Hall effect etc. Graphene, a noble 2D material with zero band gap, has been cut into nanoribbons (NRs) which develop a gap in electronic structure [1,2], thus turning into a semi-conductor. Scattering from the edges and confinement effects are the main cause of transition into semi-conducting behaviour. Quite recently, Unsal et al. [3] have presented a systematic study of ballistic transport in NRs of $HfSe_2$, together with an analysis of their thermoelectric performance. As compared to their 2D counterpart, the phononic thermal conductance of NRs was found to be suppressed by a factor of 3. Also, the p-type values of thermoelectric figure of merit were improved a lot.

Very recently, Kapoor et al. [4] have simulated the zigzag (ZZ) NRs of noble metals elements (viz. Au, Ag, Cu), and their alloys and hetero-structures modeled in the honeycomb topology. They found pristine systems metallic in nature, while alloyed ones semi-conducting, with band gap decreasing on increasing width of the NRs. Among these systems, pristine Au is predicted to have

the highest tensile strength, which decreases with width of the NR. Singh et al. [5] have calculated the phononic thermal conductance of gold and silver NRs for different widths in both ZZ and armchair (AC) configurations. For nearly the same widths, the ZZNRs show relatively higher thermal conductance. With the exception of ACNRs of Au, all other systems show a linear fit of the room temperature thermal conductance with width of the NRs.

Along the lines of phononic transport, it would be relevant to look into the electron transport properties of gold and silver NRs. Hence, in this study, we have investigated these NRs in honeycomb structure (shown in Fig. 1) for electronic transport and thermoelectric properties using the "density functional theory" (DFT) together with the "Landauer-Buttiker" (LB) approach [6,7] in linear response regime. The effect of edges and width of the NRs on transport properties is also probed.

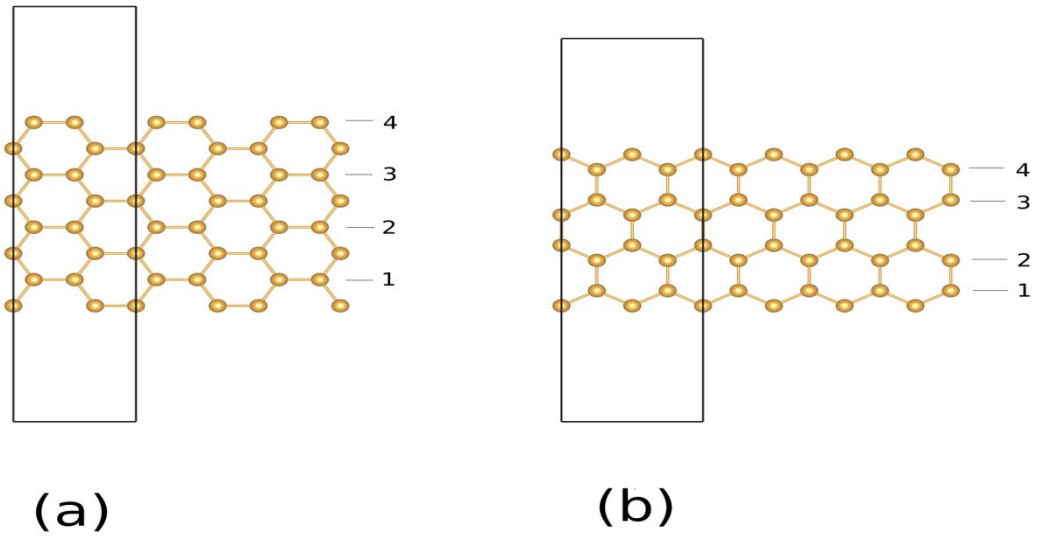

Figure 1: Ball stick depection of (a) Armchair, and (b) Zigzag gold nanoribbons with width index n=4. Rectangular box represents the unit cell chosen for the simulations.

Simulation and Modeling Details

Just like the graphene NRs, we have considered the honeycomb arrangement of atoms in the studied NRs. This leads to two different edges of the NR viz. the AC and ZZ. The width of the NR is indexed by the number of chains used to make it; for example, Fig. 1 shows the Au NRs of width index n=4 in both AC- and ZZ-configurations. The calculations for structure and electronic properties are done using the the SIESTA [8] code, a method based on DFT. Here, the norm-conserving pseudopotentials [9] based on the parameterization scheme of Troullier and Martins [10] are used, and the exchange and correlation (XC) potential is parameterized by the PBEsol-GGA functional [11]. We vary the width of NRs in the range 4-8. The periodic direction for NRs is taken to be the z-axis, while in x- and y-directions a vacuum of 20 Å is introduced. Real space integration is performed on a regular grid with a mesh cutoff of 500 Ry, while the first Brillouin zone is sampled by a uniform k-grid [12] of 1×1×30. All systems are optimized using the standard conjugate gradient (CG) technique until force on each atom becomes less than 0.04 eV/ Å. For calculating the electronic transmission function τ_{el} through the device, we have used the TBTrans utility of TranSIESTA [13,14] (a module of SIESTA) based on "non-equilibrium Green's function" (NEGF) approach [15]. We take a supercell consisting of three parts: (1) "left electrode"

(2) “right electrode”, and (3) “scattering region” (i.e., device). Each of the three regions contain one unit cell, which is the same as the one used for SIESTA calculation (see Fig. 1). First, we calculate the electrode Hamiltonian, and then repeat it three times using the SISL [16] python package. This complete Hamiltonian is fed to the TBTrans utility to calculate τ_{el}.

Results and Discussion

First, we find the relaxed positions of atoms for the chosen unit cell. Cohesive energy for these systems is found to be negative, suggesting NRs to be stable structures. The relaxed structure is used to find the electronic transmission function $\tau_{el}(E)$, plotted in Fig. 2 for increasing width of the NRs. Since the calculation of electronic transport coefficients primarily involves $\tau_{el}(E)$ near the Fermi energy E_F, we have reported it for an energy window of -0.5 to 0.5 eV about E_F. It can be seen from Fig. 2 that the ACNRs contain finite gaps in $\tau_{el}(E)$ at E_F, while the gaps disappear in the ZZ-configuration, suggesting their semi-conducting and metallic nature, respectively.

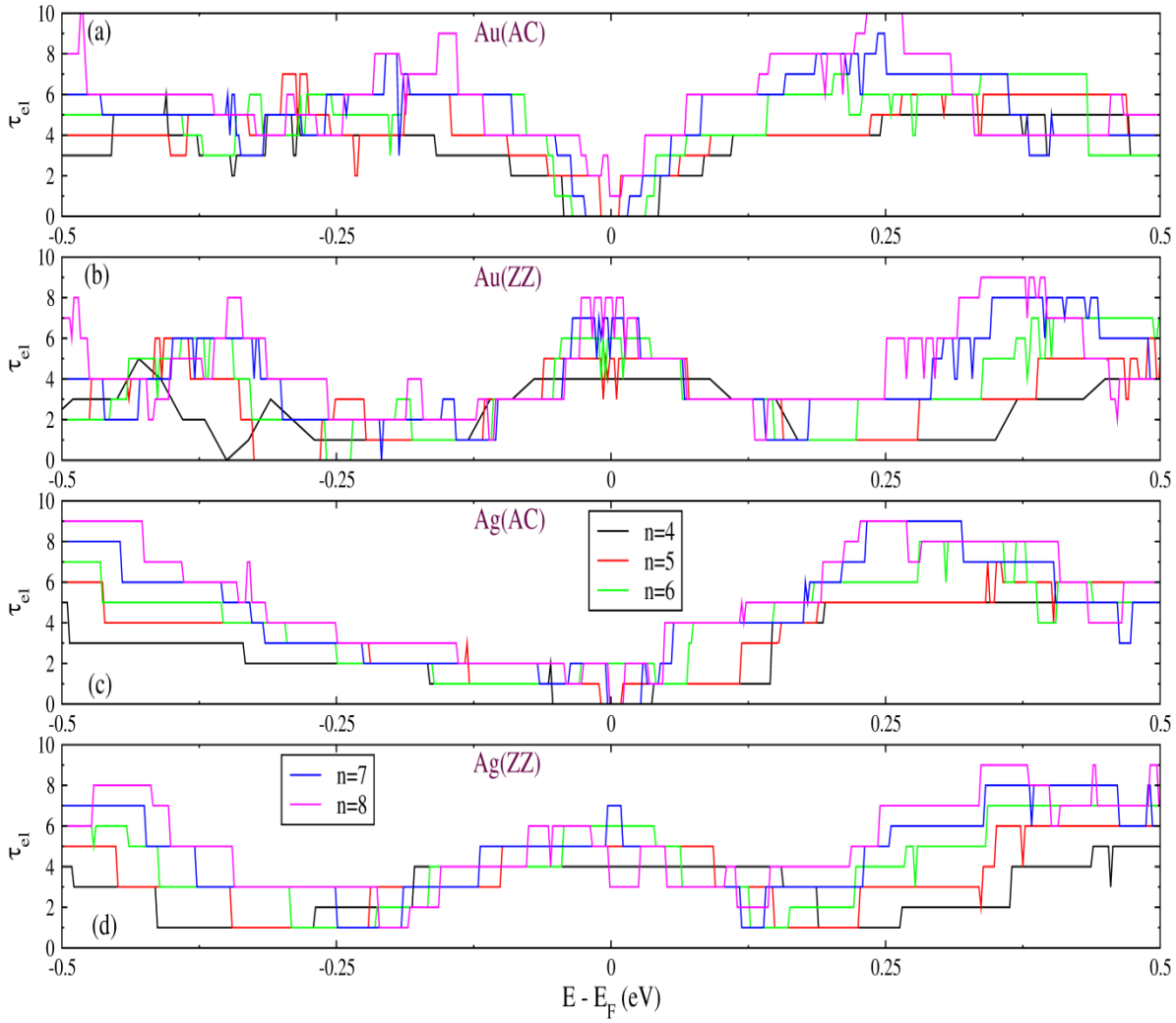

Figure 2: Calculated electronic transmission function $\tau_{el}(E)$ for (a) Au ACNRs, (b) Au ZZNRs, (c) Ag ACNRs, and (d) Ag ZZNRs systems for width index n in the range 4-8.

Materials Research Proceedings **22** (2022) 28-34 https://doi.org/10.21741/9781644901878-5

The calculated band gap values E_g of the ACNRs are summarized in Table. 1 below.

Table 1: Calculated electronic energy band gaps (in eV) in AC-configurations of NRs.

System	n=4	n=5	n=6	n=7	n=8
AuAC	0.089	0.017	0.067	0.041	-
AgAC	0.091	0.020	-	0.033	0.013

Interestingly, the systems with even width index show higher values of band gap. Also, like the atomic chains [17], the electron transport is ballistic in nature. One can obtain different transport coefficients using the LB approach by computing its main coefficient in the linear response domain as,

$$I_m(\mu,T) = \int_{-\infty}^{\infty} \tau_{el}(E)(E-\mu)^m \left(\frac{-\partial f(E,\mu,T)}{\partial E}\right) dE, \quad (1)$$

where f(E,μ,T) is the "Fermi-Dirac" distribution function, and μ and T are the average electrochemical potential and temperature of the two electrodes, respectively. From Eq. 1, we can calculate the "electrical conductance" G, the "electronic thermal conductance" κ_{el}, and the "Seebeck coefficient" S using the following relations [17],

$$G(\mu,T) = \frac{2e^2}{h} I_0(\mu,T), \quad (2)$$

$$\kappa_{el}(\mu,T) = \frac{2}{hT}\left[I_2(\mu,T) - \frac{I_1^2(\mu,T)}{I_0(\mu,T)}\right], \quad (3)$$

and,

$$S(\mu,T) = \frac{-I_1(\mu,T)}{eTI_0(\mu,T)}. \quad (4)$$

Here, h is the Planck's constant and e the electronic charge. Fig. 3 shows the calculated temperature dependence of G and κ_{el} under zero-bias condition, and the tuning of room-temperature S with electrochemical potential μ of electrodes for the considered NRs. In the systems having band gap, G starts to rise over its negligibly small value for T above a characteristic temperature E_g/k_B (typical of semi-conductors), while in metallic systems, G decreases with temperature, except for the presence of some dips (minima) or humps (maxima) (i.e., a non-monotonic dependence on T) in low temperature region. Such a non-monotonic variation in G with temperature has earlier been predicted by Singh et al. [18] for bimetallic atomic wires of noble metals. Interestingly, in Au ZZNR (n=4) and Ag ZZNRs (n=4, 5) systems, G displays a quantized behaviour up to temperatures as high as 200 K; it has values $4G_0$ and $5G_0$, respectively, for n=4 and n=5. $G_0=2e^2/h$, is the elementary quantum of electrical conductance. As can be seen from Fig. 2, this arises due to a flat and symmetric variation of $\tau_{el}(E)$ over a window of energy of order k_BT about the Fermi level E_F. On the other hand, the electronic thermal conductance κ_{el} varies non-linearly with temperature, and its magnitude increases with increasing width of the NRs. Turning to the Seebeck coefficient S, its magnitude remains negligibly small under the zero-biasing condition even for the metallic NRs. Again, this result has its origin in the flat and symmetric behaviour of $\tau_{el}(E)$ over an energy interval of order k_BT about E_F. However, S can be tuned to a great extent via biasing of electrodes. It is apparent from Fig. 3 that S oscillates with μ and even changes sign at characteristic μ. Particularly, the ACNRs show pronounced peaks for μ near either edge of gap in $\tau_{el}(E)$; for instance, S as high as -118.65 μV/K and -118.72 μV/K can be achieved at μ=0.035 eV and 0.03

eV, respectively, in the Au ACNR and Ag ACNR with n=4. As the ZZNR of Au with width n=5 develops a gap in $\tau_{el}(E)$ for μ around -0.3 eV, it also shows a significant S of 101.26 μV/K at μ= -0.32 eV. It is relevant to note here that the peak values of S in the smaller width (n=4, 5) NRs are comparable to those predicted for the atomic chains of these elements in linear, ladder and zigzag topologies [17]. Optimization of electronic thermal conductance together with its lattice counterpart, without a major change in S, can make the studied NRs useful in thermoelectric based coolers and generators. Moreover, the predicted decent values of S can be exploited for thermoelectric sensors applications.

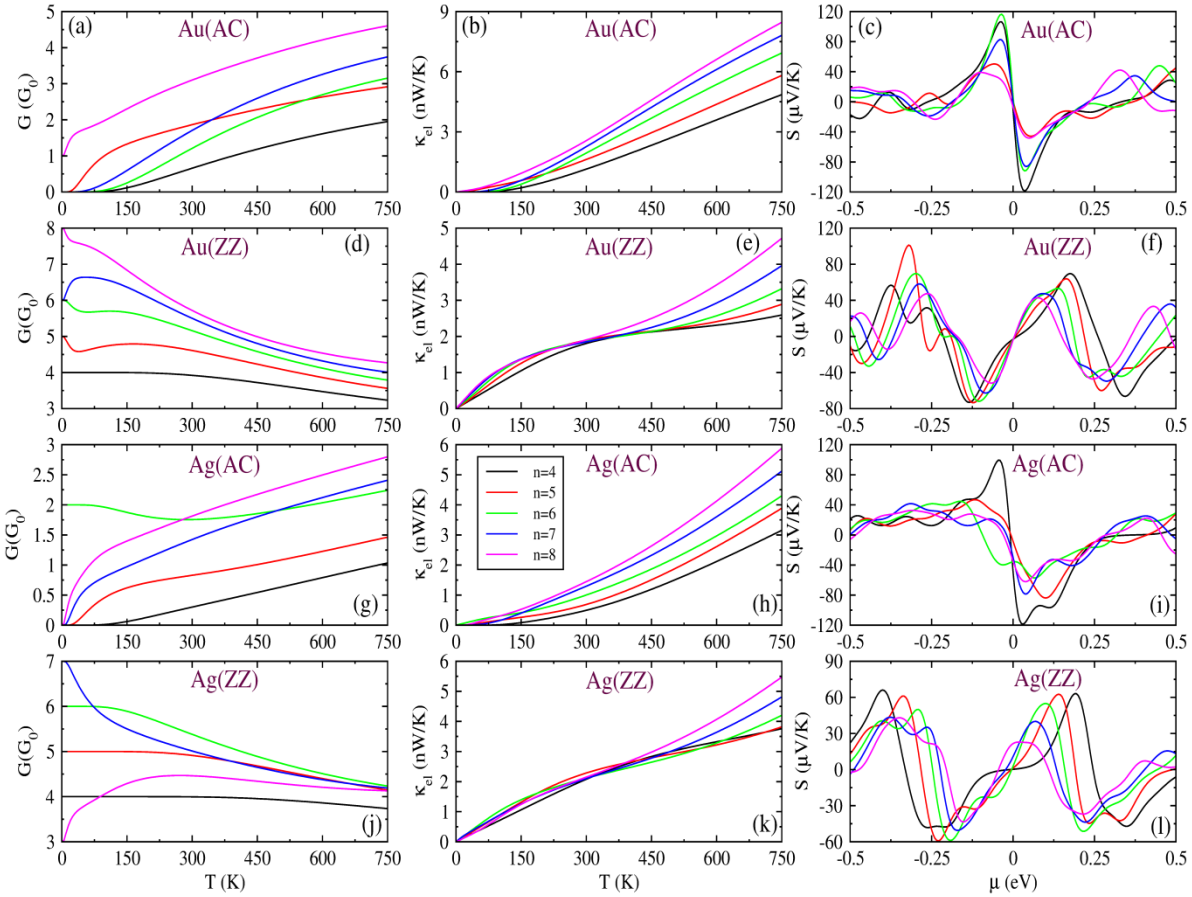

Figure 3: Variation of "electrical conductance" G, and "electronic thermal conductance" κ_{el} with temperature under zero-bias, along with the tuning of room temperature thermopower S with chemical potential μ for (a-c) Au ACNRs, (d-f) Au ZZNRs, (g-i) Ag ACNRs, and (j-l) Ag ZZNRs configurations.

Summary

To summarize, we have conducted the first-principles based simulations of ballistic electron transport in the NRs of gold and silver modeled in a topology similar to graphene NRs. For this, we have employed the NEGF approach and the "Landauer-Buttiker" formalism, with the requisite electronic structure obtained using the DFT based calculations performed with the SIESTA code. As a result of nanostructuring of monolayers along one of the lateral directions, the ACNRs become semiconducting, while the ZZNRs retain metallicity. For sufficiently small widths, the ZZNRs show a quantized electrical conductance up to temperatures as high as 200 K. Electronic heat transport exhibits a marked increase with increasing width of the NRs in AC-systems. But, in

ZZNRs, such a trend is missing for temperatures at least up to 300 K. The Seebeck coefficient S attains reasonably high values (above 100 μV/K in magnitude), when tuned via electrochemical potential μ of electrodes. Our study shows that the AC-configurations are a better candidate for thermoelectric applications.

Acknowledgements
One of the authors (SK) acknowledges Council of Scientific & Industrial Research (CSIR), New Delhi, India for providing Senior Research Fellowship (SRF).

References

[1] L. Yang, C.-H. Park, Y.-W. Son, M. L. Cohen, S. G. Louie, Quasiparticle energies and band gaps in graphene nanoribbons, Phys. Rev. Lett., 99 (2007) 186801.

[2] M. Y. Han, B. Özyilmaz, Y. Zhang, P. Kim, Energy band-gap engineering of graphene nanoribbons, Phys. Rev. Lett., 98, (2007) 206805. https://doi.org/10.1103/PhysRevLett.98.206805

[3] E. Unsal, R. Senger, H. Sevinçli, Enhancement of thermoelectric efficiency of T - $HfSe_2$ via nanostructuring, Physical Review B, 103 (2021) 014104. https://doi.org/10.1103/PhysRevB.103.014104

[4] P. Kapoor, A. Kumar, P. K. Ahluwalia, Size-dependent electronic, mechanical and optical properties of noble metal nanoribbons, Materials Science and Engineering B: Solid-State Materials for Advanced Technology, 262 (2020) 114786. https://doi.org/10.1016/j.mseb.2020.114786

[5] G. Singh, K. Kumar, R. K. Moudgil, Coherent phonon thermal transport in nanoribbons of gold and silver, in AIP conference proceedings, 2115 (2019) 030373. https://doi.org/10.1063/1.5113212

[6] M. Büttiker, Y. Imry, R. Landauer, S. Pinhas, Generalized many-channel conductance formula with application to small rings, Phys. Rev. B, 31 (1985) 6207–6215. https://doi.org/10.1103/PhysRevB.31.6207

[7] P. N. Butcher, Thermal and electrical transport formalism for electronic microstructures with many terminals, J. Phys. Condens. Matter, 2 (1990) 4869. https://doi.org/10.1088/0953-8984/2/22/008

[8] J. M. Soler, E. Artacho, J. D. Gale, A. García, J. Junquera, P. Ordejón, D. Sánchez-Portal, The SIESTA method for ab initio order-N materials simulation, Journal of Physics: Condensed Matter, 14 (2002) 2745. https://doi.org/10.1088/0953-8984/14/11/302

[9] D. R. Hamann, M. Schlüter, C. Chiang, Norm-conserving pseudopotentials, Phys. Rev. Lett., 43 (1979) 1494. https://doi.org/10.1103/PhysRevLett.43.1494

[10] N. Troullier, J. L. Martins, Efficient pseudopotentials for plane-wave calculations, Phys. Rev. B, 43 (1991) 1993. https://doi.org/10.1103/PhysRevB.43.1993

[11] J. P. Perdew, K. Burke, M. Ernzerhof, Generalized gradient approximation made simple, Phys. Rev. Lett., 77 (1996) 3865. https://doi.org/10.1103/PhysRevLett.77.3865

[12] J. Moreno, J. M. Soler, Optimal meshes for integrals in real- and reciprocal-space unit cells, Phys. Rev. B, 45 (1992) 13891. https://doi.org/10.1103/PhysRevB.45.13891

[13] M. Brandbyge, J.-L. Mozos, P. Ordejón, J. Taylor, K. Stokbro, Density-functional method for nonequilibrium electron transport, Phys. Rev. B, 65 (2002) 165401. https://doi.org/10.1103/PhysRevB.65.165401

[14] N. Papior, N. Lorente, T. Frederiksen, A. García, M. Brandbyge, Improvements on non-equilibrium and transport Green function techniques: The next-generation transiesta, Computer Physics Communications, 212 (2017) 8. https://doi.org/10.1016/j.cpc.2016.09.022

[15] S. Datta, Electronic Transport in Mesoscopic Systems, Cambridge university press, 1997.

[16] N. Papior, Sisl: v.0.10.0, 2020.

[17] G. Singh, K. Kumar, R. K. Moudgil, On topology-tuned thermoelectric properties of noble metal atomic wires, Physica E: Low-dimensional Systems and Nanostructures, 109 (2019) 114. https://doi.org/10.1016/j.physe.2019.01.007

[18] G. Singh, K. Kumar, R. K. Moudgil, Alloying-induced spin Seebeck effect and spin figure of merit in Pt-based bimetallic atomic wires of noble metals, Phys. Chem. Chem. Phys., 21 (2019) 20965. https://doi.org/10.1039/C9CP01671F